Mineralization of Self-assembled Peptide Nanofibers for Rechargeable Lithium Ion Batteries

By *Jungki Ryu, Sung-Wook Kim, Kisuk Kang,** and *Chan Beum Park**

One of most unique and fascinating features of natural biomineralization processes is the controlled growth and hierarchical organization of inorganic minerals along with organic materials. Such marvels of nature give excellent physicochemical properties to natural biomaterials[1–3] and provide inspiration for the synthesis of novel functional nanomaterials to chemists and materials scientists.[4–9] For example, natural bones with excellent mechanical properties are a kind of organic/inorganic hybrid materials with organic collagen nanofibrils and inorganic calcium phosphate nanocrystals hierarchically organized on a nanoscale.[10] Researchers have found that the hierarchical organization of organic and inorganic components of natural biomaterials is due mainly to the repetitive display of acidic functional groups on the surface of organic materials[2,11] that can act as a nucleation site for the growth of inorganic materials. In this regard, numerous efforts have been made to synthesize novel hybrid nanomaterials by mimicking biomineralization processes especially for biomedical applications.[12–15] For example, Hartgerink and colleagues reported on synthesis and mineralization of peptide-amphiphile nanofibers displaying phosphate groups on their surface for bone regeneration.[13] To date, however, the synthesis of industrially important hybrid nanomaterials by mimicking biomineralization processes has been rarely reported despite many potential advantages of biomimetic approaches such as environmental compatibility and high controllability of shape and size.

On the other hand, interest is growing in the fabrication of functional nanomaterials by self-assembly of peptide-based building blocks because of functional flexibility and environmental compatibility.[16,17] Among numerous self-assembling peptides reported to date, diphenylalanine (Phe-Phe, FF) and its derivatives[18–30] are simplest peptides exhibiting unique mechanical,[19] electrochemical,[20] and optical properties[21] as well as high thermal and chemical stabilities.[23] It has been reported that they can readily form various nanostructures, including nanotubes,[18–22] nanowires,[23–27] nanospheres,[28] organogels,[29] and hydrogels[30] through a self-assembly process. Here, we first report the synthesis of transition metal phosphate nanotubes for application as a cathode material for rechargeable lithium (Li) ion batteries by using a peptide hydrogel self-assembled from fluorenylmethoxycarbonyl (Fmoc)-FF[30] as a template. The peptide hydrogel is composed of very thin nanofibers (diameter about a few tens of nm) and displays numerous acidic and polar moieties on its surface (Figures S1 and S2 in the Supporting Information), which are highly beneficial for the synthesis of novel organic/inorganic hybrid nanomaterials.

We synthesized peptide/transition metal phosphate core/shell nanofibers, as schematically illustrated in **Figure 1a**. Peptide nanofibers that could act as a mineralization template were prepared by the self-assembly of Fmoc-FF peptide (Figure 1b) in an aqueous solution. Briefly, a clear peptide solution was prepared by dissolving the peptide in 1,1,1,3,3,3-hexafluoro-2-propanol (100 mg mL^{-1}) and then diluting with deionized water to a concentration of 2 mg mL^{-1} to form a transparent hydrogel composed of physically crosslinked peptide nanofibers (Figures 1c and d). According to scanning electron microscopy (SEM), peptide nanofibers are 10–20 nm wide and several tens of μm long (Figure 1c). The prepared peptide hydrogel was then mineralized with transition metal phosphate by sequentially treating with 10 mM MCl_x (M = Fe, Co, Cu, Ni, or Mn) solution in deionized water (pH < 3.0) and 10 mM NaH_2PO_4 solution in 50 mM Tris (pH 7.0) using a vacuum filtration apparatus (Figure 1a). The mineralization process was repeated several times to completely coat the peptide nanofibers with transition metal phosphate minerals.

After successively treating with transition metal cations and phosphate anions, we found significant changes in the properties and morphologies of peptide nanofibers (see Figure S3 in the Supporting Information). After the treatment, peptide nanofibers exhibited unique colors depending on the type of metal ions treated (Figure S1a). For example, the color of dried peptide nanofibers changed from white to brown after treatment with Fe^{3+} and PO_4^{3-} ions. In addition, peptide nanofibers no longer showed characteristics of a hydrogel after the treatment, e.g., a reduced capacity for water absorption, which we attribute to the burial of hydrophilic residues by the formation of transition metal phosphate minerals on the surface of peptide nanofibers. SEM and transmission electron microscopy (TEM) confirmed the formation of inorganic materials along the peptide nanofibers (Figures 1c–f and Figure S3 in the Supporting Information). The surface of peptide nanofibers was initially smooth but became very rugged after the treatment irrespective of metal ions used (Figures S3b–f). High-magnification TEM and SEM analysis showed that the rugged surface was caused by the formation of inorganic nanoparticles along the peptide nanofibers (Figures 1c–f). Selected-area electron diffraction (SAED) analysis and elemental analysis by energy dispersive X-ray spectroscopy (EDS) revealed that inorganic nanoparticles were amorphous transition metal phosphate (Figures 1f inset and 1g).

[*] J. Ryu, S.-W. Kim, Prof. K. Kang, Prof. C. B. Park
Department of Materials Science and Engineering
Korea Advanced Institute of Science and Technology (KAIST)
335 Science Road, Daejeon 305-701 (Republic of Korea)
E-mail: parkcb@kaist.ac.kr; matlgen1@kaist.ac.kr

DOI: 10.1002/adma.201000669

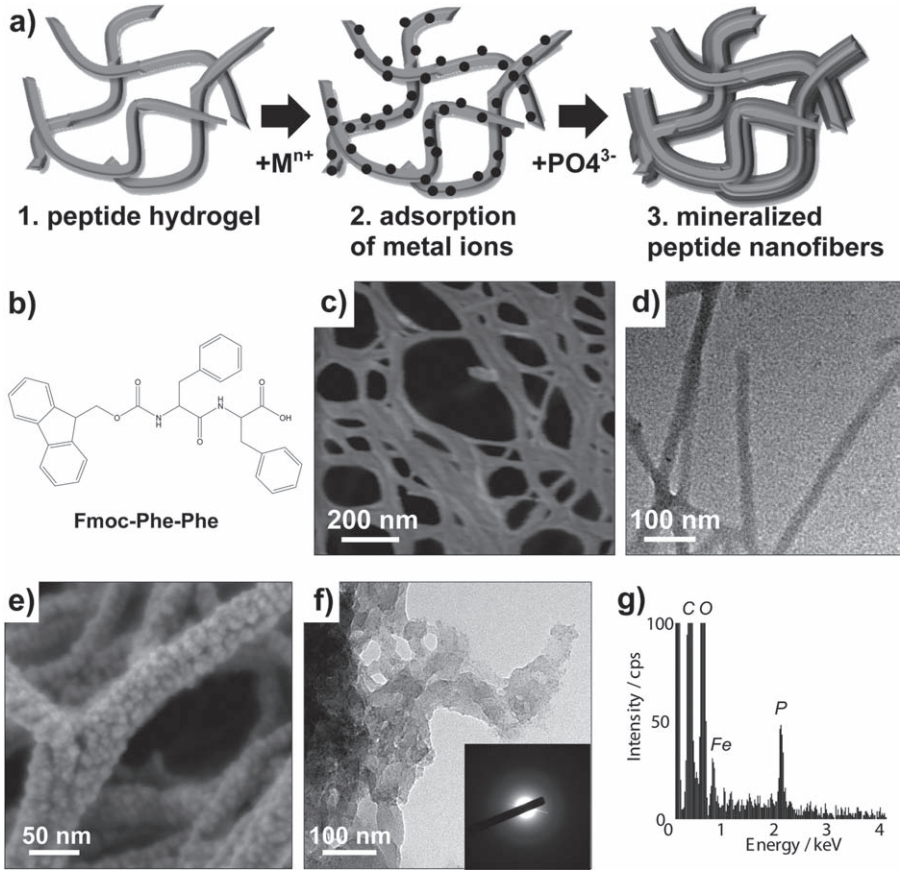

Figure 1. Fabrication of nanostructured transition metal phosphates by biomimetic mineralization of peptide nanofibers. a) Sequential treatment of peptide nanofibers, which are formed by self-assembly of Fmoc-diphenylalanine (b), with aqueous solutions containing transition metal cations and phosphate anions led to the formation of peptide/transition metal phosphate core/shell nanofibers. For example, peptide nanofibers (c,d) are readily coated with irregularly shaped amorphous $FePO_4$ (e,f) after successive treatment with Fe^{3+} and PO_4^{3-} ions as evidenced by SEM (c,e) and TEM (d,f) observations,SAED inset), and EDS analysis (g). Note that the appearance of diffuse rings in the SAED pattern indicates the formation of amorphous $FePO_4$.

Mineralized peptide nanofibers were further investigated with differential scanning calorimetry (DSC), thermogravimetric analysis (TGA), and Fourier transform infrared (FT-IR) spectroscopy. We focused particularly on the mineralization of peptide nanofibers with $FePO_4$ that has diverse applications in energy storage[9,31–34] and catalysis.[35,36] DSC (Figure S4 in the Supporting Information) and TGA (Figure S5 in the Supporting Information) analysis suggested that minerals that had formed along the peptide nanofibers were amorphous, hydrated $FePO_4$ (i.e., $FePO_4{\cdot}nH_2O$). Both pristine and mineralized peptide nanofibers exhibited an endothermic DSC peak and a slight weight decrease at around 90 °C, which should originate from the evaporation of water molecules adsorbed on the surface of nanofibers. For mineralized nanofibers, several additional peaks appeared at around 140 and 430 °C, which can be attributed to the dehydration of amorphous hydrated $FePO_4$ ($FePO_4{\cdot}nH_2O \rightarrow FePO_4$) and to the phase transformation of $FePO_4$ from amorphous (a-$FePO_4$) to hexagonal crystalline phase, respectively.[33] From TGA thermograms of peptide nanofibers, we were able to calculate the relative amounts of peptide nanofibers and $FePO_4$ minerals. Compared with pristine peptide nanofibers, $FePO_4$-coated peptide nanofibers (prepared by repeating the mineralization process six times) additionally lost 10% of weight in the temperature range from room temperature to 200 °C. Considering that $FePO_4$ normally has a dihydrate form (i.e., $FePO_4{\cdot}2H_2O$) when synthesized in aqueous solution at room temperature[37] and the theoretical weight loss upon dehydration of pure $FePO_4{\cdot}2H_2O$ is 19.2%, the $FePO_4{\cdot}2H_2O$ mineral component accounts for about 52% of the total weight of mineralized peptide nanofibers (weight ratio of $FePO_4{\cdot}2H_2O$/peptide ≈ 1.08). When we further studied the effect of the number of repeated mineralization processes on the amount of mineral components, we found it was saturated after about six replications of mineralization processes (Figure S6 in the Supporting Information), implying that functional groups displayed on the surface of peptide nanofibers in a regular repetitive pattern have a critical role in the mineralization of the nanofibers. This also indicates that the thickness of the inorganic sheath can be controlled.

We further confirmed the formation of $FePO_4$ minerals on the surface of peptide nanofibers by using FT-IR spectroscopy (Figure S7 in the Supporting Information). Both pristine and mineralized peptide nanofibers exhibited absorption peaks at around 1658 and 1696 cm^{-1}, indicating that the peptide adopts

a β-sheet conformation.[30] For mineralized peptide nanofibers, an additional peak originating from Fe–O–P vibration was observed at around 1043 cm^{-1}.[38,39] It is noted that results of FT-IR spectroscopic analysis (see also Figures S1 and F2 in the Supporting Information) were consistent with a recent report by Smith et al.[30] suggesting that Fmoc-FF forms peptide nanofibers adopting β-sheet conformation through self-assembly driven by π–π stacking interactions. According to the report, the molecular arrangement in the Fmoc-FF nanofibers reflects polar and acidic moieties, such as carboxyl and amide groups, exposed on the surface of peptide nanofibers in a regular repetitive pattern. Considering that a number of biological molecules and artificial biomaterials known to possess biomineralization activity commonly have acidic moieties (e.g., phosphate, sulfate, and carboxylate) displayed on their surface in a regular pattern,[2,11,13] we speculate that the surface-exposed acidic and polar groups are responsible for the formation and growth of transition metal phosphate minerals along the peptide nanofibers in the present study.

We could readily fabricate $FePO_4$ nanotubes coated with residual conductive carbon layers by treating the peptide/$FePO_4$ core/shell nanofibers at moderately high temperature. $FePO_4$ minerals remained amorphous with dehydration when incubated at 350 °C (Figure S8 in the Supporting Information), whereas Fmoc-FF transformed into amorphous carbon layers by thermal decomposition (**Figure 2a**). According to previous reports, trigonal[39] and hexagonal[33] $FePO_4$ phases are electrochemically inactive, but dehydrated amorphous $FePO_4$ has a higher theoretical capacity[40] and better cyclability than hydrated $FePO_4$ as a Li ion battery cathode.[33] In addition, the amorphous nature of $FePO_4$ nanotubes can be beneficial for ensuring more reliable electrochemical performance because amorphous phase is conceptually free of stress originating from lattice mismatch that is frequently observed at the phase boundary of crystalline materials during charge and discharge processes. After carbonization of the peptide core, a color change was observed from brown to black. A hollow tubular structure with an average diameter of 20 nm and wall thickness of 5 nm was clearly visible in electron micrographs (Figure 2b–d). The $FePO_4$ nanotubes were interconnected forming a three-dimensional network structure, which is beneficial for electrode performance because it improves electronic conductivity and structural integrity.[41] Further analysis by FT-IR spectroscopy (Figure 2e) confirmed that $FePO_4$ nanotubes were coated with carbon layers. A sp^2 carbon peak located around 1620 cm^{-1} can be attributed to the formation of amorphous graphitic carbon layers.

Based on the results, we attempted to apply the carbon-coated $FePO_4$ nanotubes in Li ion battery applications. Recently, bulk $FePO_4$ has been extensively investigated as a next-generation cathode material in Li ion batteries, but critical problems have been revealed such as low electronic conductivity and slow insertion/extraction rate of Li ion.[42] The use of nanostructured $FePO_4$ coated with conductive materials has been suggested to solve such intrinsic problems;[9,31] however, only a few reports

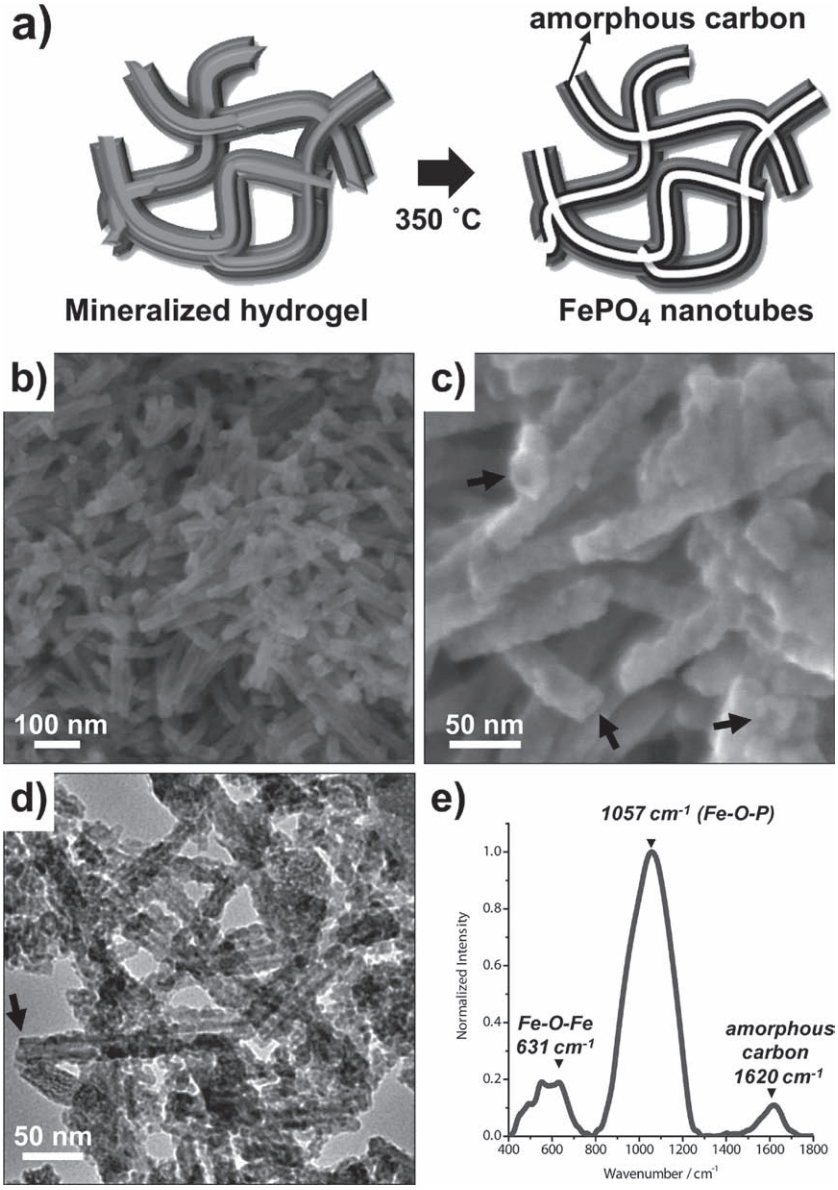

Figure 2. Synthesis of $FePO_4$ nanotubes by heat treatment of peptide/$FePO_4$ hybrid nanofibers. a) Peptide nanofibers mineralized with $FePO_4$ were treated at 350 °C to carbonize the peptide core and thus to fabricate hollow $FePO_4$ nanotubes with inner walls coated with a thin layer of conductive carbon. Tubular structures are clearly visible in SEM (b–c) and TEM (d) micrographs. e) FT-IR spectroscopy confirmed carbonization of the peptide core. Note that a peak at approximately 1620 cm^{-1} is attributed to vibrations of sp^2 carbon, indicating the formation of amorphous graphitic carbon. Arrows indicate the openings of $FePO_4$ nanotubes.

have been published on the synthesis and characterization of nanostructured $FePO_4$, mostly in the form of nanoparticles, because of difficulties in synthesis. Here, we tested the electrochemical performance of carbon-coated $FePO_4$ nanotubes as a positive electrode for Li ion batteries by examining charge/discharge behavior. It is expected that the electrochemical performance could be improved because carbon layers can offer enhanced electronic conduction and adhesion for $FePO_4$ nanocrystallites and nanotubes. We constructed a Swagelok-type test cell by using Li metal and $FePO_4$ nanotubes as a counter and working electrode, respectively, separated by a porous polymer membrane filled with a liquid electrolyte of 1 M $LiPF_6$ in a 1:1 mixture of ethylene carbonate and dimethyl carbonate. Figure S9 (in the Supporting Information) shows a cyclic voltammogram of the nanotubular $FePO_4$. The voltammogram exhibits a pair of anodic and cathodic peaks near 3 V versus Li^+/Li, corresponding to a Fe^{3+}/Fe^{2+} redox couple, which is associated with insertion and extraction of Li^+ ions.[33] **Figure 3** shows discharge–charge curves of carbon-coated $FePO_4$ nanotubes upon cycling. The $FePO_4$ nanotubes exhibited a specific capacity of approximately 170 mAh g^{-1} in the first cycle, close to its maximum theoretical capacity (178 mAh g^{-1}),[40] and a highly reversible capacity of about 150 mAh g^{-1} after the second cycle with a coulombic efficiency near 100%. Upon discharge, monotonic decrease of voltage occurred, a characteristic of amorphous $FePO_4$. This monotonic decrease of voltage should be beneficial for monitoring the state of charge of Li ion batteries without a plateau region.[33,37] In order to support our hypothesis that the carbonization of peptide core improves the electrochemical performance, we observed the first discharge capacity of hydrogel-$FePO_4$ composite in comparison with that of $FePO_4$ nanotubes having carbon layers. As shown in Figure S10 (in the Supporting Information), $FePO_4$ nanotubes with carbon layers showed much higher capacity, which indicates that amorphous carbon layers effectively enhanced the electrochemical performance of $FePO_4$-based electrode material.

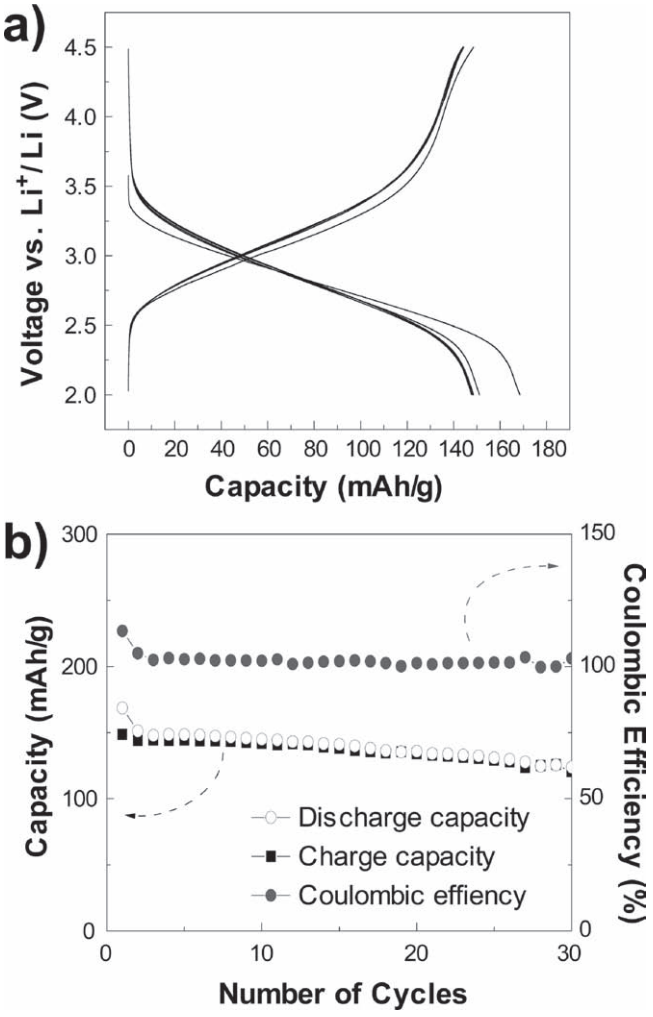

Figure 3. Electrochemical performance of $FePO_4$ nanotubes as a cathode material for rechargeable Li ion batteries. Plots showing discharge-charge curves of 1–5 cycles (a) and capacity retention of $FePO_4$ nanotubes with a current rate of 10 mA g^{-1} (b).

Compared with previously reported $FePO_4$ nanostructures, we found that our $FePO_4$ nanotubes performed very well as a cathode material for rechargeable Li ion batteries in terms of specific capacity and capacity retention. We believe the anisotropic structure of $FePO_4$ nanotubes as well as their small dimension and carbon coating are partly responsible for their excellent electrochemical performance. Bruce et al. recently argued in their review article[41] that anisotropic nanomaterials are more attractive than isotropic nanoparticles because one long dimension and two short dimensions simultaneously ensure good electronic transport and fast Li ion diffusion, respectively. The three-dimensional network structures of nanotubes are also believed to provide an additional advantage of the structural stability of $FePO_4$ cathode during cycles, ensuring stable capacity retention. Furthermore, compared with conventional methods used in the synthesis of transition metal phosphate nanostructures, our approach utilizing the biomimetic mineralization of peptide nanofibers is environmentally friendly as it requires no additional chemicals such as urea or hydrofluoric acid. For example, Chen et al. recently reported the synthesis of colloidal particles of various transition metal phosphates without template materials by controlling precipitation reactions between transition metal cations and phosphate anions with urea, which is hydrolyzed into toxic ammonium ions.[43] It may be possible to avoid the use of urea by using porous template materials such as mesoporous silica, porous aluminum oxide, and polymer membrane, but the removal of electrochemically inactive template materials still requires the use of strong acids (e.g., hydrofluoric acid) or toxic organic solvents. In contrast, our approach requires only precursor chemicals, such as metal chloride salts and sodium phosphate, dissolved in aqueous solution for the synthesis of anisotropic transition metal phosphate nanostructures. The advantages of our approach become more evident considering that the peptide core can be readily removed and converted into a conductive carbon layer by heat treatment,

In summary, we synthesized nanostructured transition metal phosphate via biomimetic mineralization of peptide nanofibers. Fmoc-FF peptides self-assembled into nanofibers displaying numerous acidic and polar moieties on their surface and readily mineralized with transition metal phosphate by sequential

treatment with aqueous solutions containing transition metal cations and phosphate anions. For Li ion battery applications, we focused on the synthesis of $FePO_4$ nanostructures; $FePO_4$-mineralized peptide nanofibers were treated at 350 °C to fabricate $FePO_4$ nanotubes with inner walls coated with a thin layer of conductive carbon by carbonization of the peptide core. The carbon-coated $FePO_4$ nanotubes were found to be a promising cathode material for rechargeable Li ion batteries with a high reversible capacity and good capacity retention during cycling.

Supporting Information

Supporting Information is available from the Wiley Online Library or from the author.

Acknowledgements

S.-W.K and J. R. contributed equally to this work. This study was supported by grants from the National Research Foundation (NRF) National Research Laboratory (R0A-2008-000-20041-0; C. B. P.), Engineering Research Center (2008-0062205; C. B. P.), Converging Research Center (2009-0082276; C. B. P.), and WCU (31-2008-000-10055-0; K. K.) programs. This research was supported by Energy Resource Technology R&D Program (20092020100040; K. K.) funded by the Ministry of Knowledge Economy, Republic of Korea. This work was also supported by the National Research Foundation (NRF) Grant funded by the Korean Government (MEST) (NRF-2009-0094219; K. K.).

Received: February 23, 2010
Revised: March 18, 2010
Published online: July 26, 2010

[1] L. Addadi, S. Weiner, *Nature* **1997**, *389*, 912.
[2] S. Weiner, L. Addadi, *J. Mater. Chem.* **1997**, *7*, 689.
[3] S. Mann, *Biomineralization: principles and concepts in bioinorganic materials chemistry* Oxford University Press, New York **2001**.
[4] S. Mann, *Nature* **1993**, *365*, 499.
[5] M. Sarikaya, C. Tamerler, A. K.-Y. Jen, K. Schulten, F. Baneyx, *Nat. Mater.* **2003**, *2*, 577.
[6] T.-X. Fan, S.-K. Chow, D. Zhang, *Prog. Mater. Sci.* **2009**, *54*, 542.
[7] S. Nikolov, M. Petrov, L. Lymperakis, M. Friak, C. Sachs, H.-O. Fabritius, D. Raabe, J. Neugebauer, *Adv. Mater.* **2010**, *22*, 519.
[8] K. T. Nam, D.-W. Kim, P. J. Yoo, C.-Y. Chiang, N. Meethong, P. T. Hammond, Y.-M. Chiang, A. M. Belcher, *Science* **2006**, *312*, 885.
[9] Y. J. Lee, H. Yi, W.-J. Kim, K. Kang, D. S. Yun, M. S. Strano, G. Ceder, A. M. Belcher, *Science* **2009**, *324*, 1051.
[10] S. Weiner, H. D. Wagner, *Annu. Rev. Mater. Sci.* **1998**, *28*, 271.
[11] M. B. Dickerson, K. H. Sandhage, R. R. Naik, *Chem. Rev.* **2008**, *108*, 4935.
[12] J. Aizenberg, *Adv. Mater.* **2004**, *16*, 1295.
[13] J. D. Hartgerink, E. Beniah, S. I. Stupp, *Science* **2001**, *294*, 1684.
[14] Z. A. C. Schnepp, R. Gonzalez-McQuire, S. Mann, *Adv. Mater.* **2006**, *18*, 1869.
[15] L. C. Palmer, C. J. Newcomb, S. R. Kaltz, E. D. Spoerke, S. I. Stupp, *Chem. Rev.* **2008**, *108*, 4754.
[16] S. Zhang, *Nat. Biotechnol.* **2003**, *21*, 1171.
[17] X. Gao, H. Matsui, *Adv. Mater.* **2005**, *17*, 2037.
[18] M. Reches, E. Gazit, *Science* **2003**, *300*, 625.
[19] L. Niu, X. Chen, S. Allen, S. J. B. Tendler, *Langmuir* **2007**, *23*, 7443.
[20] M. Yemini, M. Reches, J. Rishpon, E. Gazit, *Nano Lett.* **2005**, *5*, 183.
[21] J. Ryu, S. Y. Lim, C. B. Park, *Adv. Mater.* **2009**, *21*, 1577.
[22] S.-W. Kim, T. H. Han, J. Gwon, H.-S. Moon, S.-W. Kang, S. O. Kim, K. Kang, *ACS Nano* **2009**, *3*, 1085.
[23] J. Ryu, C. B. Park, *Biotechnol. Bioeng.* **2010**, *105*, 221.
[24] J. Ryu, C. B. Park, *Adv. Mater.* **2008**, *20*, 3754.
[25] J. Ryu, C. B. Park, *Angew. Chem. Int. Ed.* **2009**, *48*, 4820.
[26] J. S. Lee, J. Ryu, C. B. Park, *Soft Matter* **2009**, *5*, 2717.
[27] J. Ryu, S.-W. Kim, K. Kang, C. B. Park, *ACS Nano* **2010**, *4*, 159.
[28] X. Yan, Q. He, K. Wang, L. Duan, Y. Cui, Y. Li, *Angew. Chem. Int. Ed.* **2007**, *46*, 2431.
[29] X. Yan, Y. Cui, Q. He, K. Wang, J. Li, *Chem. Mater.* **2008**, *20*, 1522.
[30] A. M. Smith, R. J. Williams, C. Tang, P. Coppo, R. F. Collins, M. L. Turner, A. Saiani, R. V. Ulijn, *Adv. Mater.* **2008**, *20*, 37.
[31] J.-M. Tarascon, M. Armand, *Nature* **2001**, *414*, 359.
[32] M. Armand, J.-M. Tarascon, *Nature* **2008**, *451*, 652.
[33] Y.-S. Hong, K. S. Ryu, Y. J. Park, M. G. Kim, J. M. Lee, S. H. Chang, *J. Mater. Chem.* **2002**, *12*, 1870.
[34] M. S. Whittingham, *Chem. Rev.* **2004**, *104*, 4271.
[35] D. Yu, J. Qian, N. Xue, D. Zhang, C. Wang, X. Guo, W. Ding, Y. Chen, *Langmuir* **2007**, *23*, 382.
[36] M. W. Kanan, D. G. Nocera, *Science* **2008**, *321*, 1072.
[37] C. Delacourt, P. Poizot, D. Bonnin, C. Masquelier, *J. Electrochem. Soc.* **2009**, *156*, A595.
[38] S. Okada, T. Yamamoto, Y. Okazaki, J.-I. Yamaki, M. Tokunaga, T. Nishida, *J. Power Sources* **2005**, *146*, 570.
[39] Z. C. Shi, A. Attia, W. L. Ye, Q. Wang, Y. X. Li, Y. Yang, *Electrochim. Acta* **2008**, *53*, 2665.
[40] C. Gerbaldi, G. Meligrana, S. Bodoardo, A. Tuel, N. Penazzi, *J. Power Sources* **2007**, *174*, 501.
[41] P. G. Bruce, B. Scrosati, J.-M. Tarascon, *Angew. Chem. Int. Ed.* **2008**, *47*, 2930.
[42] S.-Y. Chung, J. T. Bloking, Y.-M. Chiang, *Nat. Mater.* **2002**, *1*, 123.
[43] C. Chen, W. Chen, J. Lu, D. Chu, Z. Huo, Q. Peng, Y. Li, *Angew. Chem. Int. Ed.* **2009**, *48*, 4816.